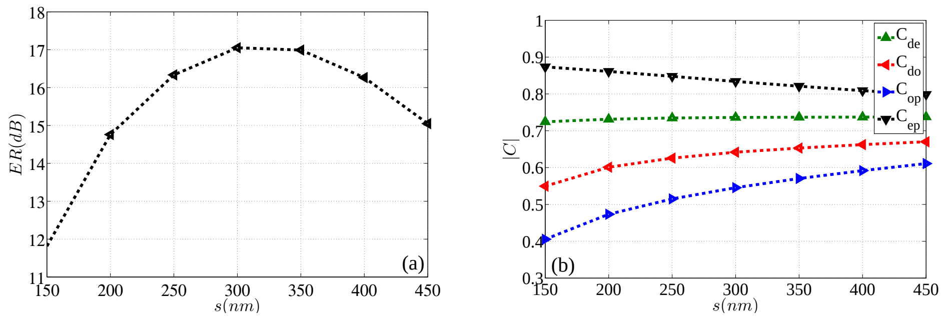

Fig. 7. Extinction ratio (ER) and amplitude of the coupling coefficient $|C|$ versus the arm separation (s) when the field is excited by the dielectric mode.

eigenmodes have different amplitudes due to the unequal excitation and experience different losses due to different field distributions. Consequently, the two eigenmodes will never be able to completely cancel each other, thus leading to a crosstalk [22]. The extinction ratio, which is defined as the ratio of maximum output power from the plasmonic arm to minimum output power from the dielectric arm when the input is fed from the dielectric arm, can be used to characterize the cross-talk of this directional coupler. From Eqs. (3) and (4), the extinction ratio (ER) can be approximated as:

$$ER = 20\times\lg\left|\frac{|C_{de}C_{ep}|\,e^{-\beta_{ei}L_c}e^{i\left(\beta_{er}L_c+\theta_{de}+\theta_{ep}\right)}+|C_{do}C_{op}|\,e^{-\beta_{oi}L_c}e^{i\left(\beta_{or}L_c+\theta_{do}+\theta_{op}\right)}}{|C_{de}C_{ed}|\,e^{-\beta_{ei}L_c}e^{i(\beta_{er}L_c+\theta_{de}+\theta_{ed})}+|C_{do}C_{od}|\,e^{-\beta_{oi}L_c}e^{i(\beta_{or}L_c+\theta_{do}+\theta_{od})}}\right| \qquad (5)$$

The extinction ratio of the hybrid coupler versus the arm separation is shown in Fig. 7(a). The extinction ratio exceeds 10 dB in the whole range of interest. At s=250 nm, the extinction ratio is around 16 dB. The maximum extinction ratio is 17 dB, which occurs at s=300 nm. The extinction ratio degrades with a decreasing s at $s<300$ nm. This is mainly caused by the unequal excitation of the quasi-even and quasi-odd eigenmodes at z=0. Figure 7(b) shows coupling coefficients of the dielectric mode to the two eigenmodes ($|C_{de}|$ and $|C_{do}|$) and those of the two eigenmodes to the plasmonic mode ($|C_{ep}|$ and $|C_{op}|$). It can be seen that the difference between $|C_{de}|$ and $|C_{do}|$ increases with the decreasing s. Therefore, the excited quasi-even and quasi-odd eigenmodes are unequal, thus causing the extinction ratio degradation at small s. When $s>350$ nm, the extinction ratio degrades with an increasing s, which is mainly caused by the increase in the coupling length. The coupling length increases exponentially with s and thus the propagation loss increases correspondingly, thereby degrading the extinction ratio at large s.

4.3. Insertion loss

The total insertion loss of the hybrid coupler consists of three parts: the coupling loss at the input end (in-coupling loss), the coupling loss at the output end (out-coupling loss) and the propagation loss for one coupling length in the coupler. These three types of losses and the total insertion loss of the coupler are shown in Fig. 8(a). The in-coupling loss and the out-coupling loss are below 1 dB in the whole range of interest and can be even neglected at large s. Figure 8(b) shows the decoupled dielectric field and the coupled field along x=0 at z=0. It can be seen that the coupled field at z=0 doesn't totally agree with the decoupled dielectric field due to the introduction of the plasmonic arm, which causes the in-coupling loss. Similarly, the difference between the coupled field at z=L_c and decoupled plasmonic field accounts for the out-coupling loss at z=L_c, which is shown in Fig. 8(c). Both the in-coupling and out-coupling

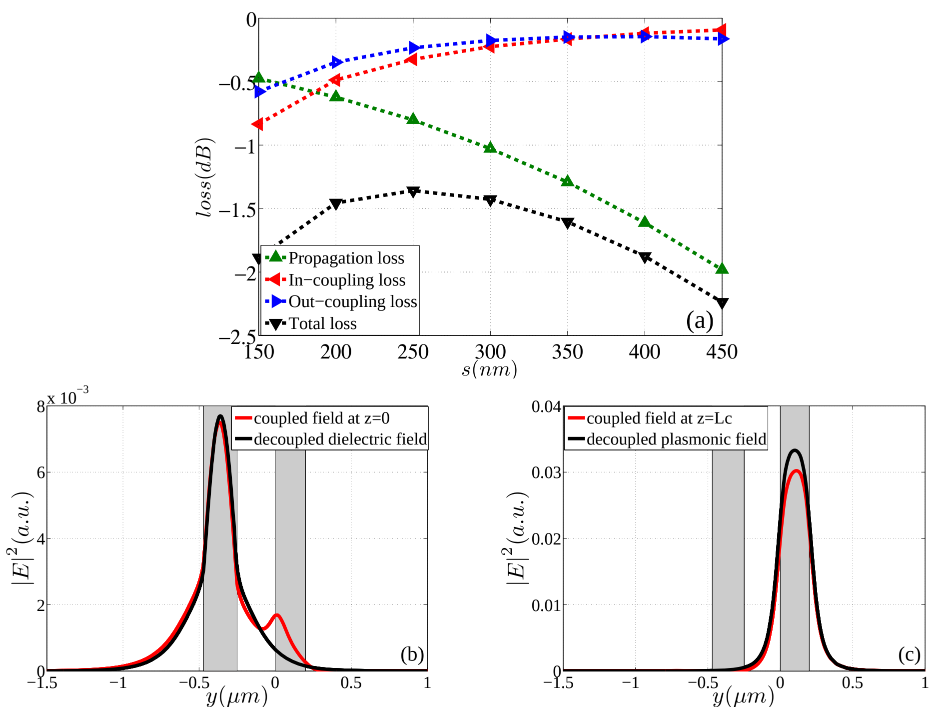

Fig. 8. (a) Losses versus the arm separation (*s*). (b) Comparison of the input dielectric electric field intensity and the coupled electric field intensity along *x*=0 at *z*=0. (c) Comparison of the output plasmonic electric field intensity and the coupled electric field intensity along *x*=0 at *z*=L_c. The fields are excited by the dielectric modes at *s*=250 nm. The dashed lines in (b) and (c) indicate the boundaries of both arms.

loss decrease when *s* increases. This is reasonable since the coupling becomes weak at large *s* and thus the in-coupling and out-coupling of the field are less affected by the other waveguide. The propagation loss in the coupler increases exponentially with *s*, which is mainly caused by the increase in the coupling length. At *s*>300 nm, the propagation loss dominates the insertion loss. The minimum insertion loss is -1.4 dB, which occurs at *s*=250 nm.

Since the hybrid directional coupling can be utilized to efficiently excite the MIM plasmonic mode with the dielectric mode, it becomes necessary to analyze the coupling efficiency of the hybrid coupler. The coupling efficiency is defined as the percentage of maximum output power from the plasmonic waveguide with respect to the input power into the dielectric waveguide. The coupling efficiency (η) can be related to the insertion loss (in dB) by $\eta = 10^{\alpha/10}$. The obtained maximum coupling efficiency is 73% at *s*=250 nm.

4.4. Tolerance to the structural parameters of the plasmonic waveguide

For a directional coupler, structural parameters are quite critical in making the propagation constants of the two arms match each other. Therefore, the tolerance of the coupler to the structural parameters are usually very tight. However, for the hybrid coupler proposed here, it shows high tolerance to the structural parameters of the plasmonic waveguide, thus alleviating the stringent requirements in fabrications to some extent. Figures 9(a)-(c) show the tolerance of the coupling length, extinction ratio and insertion loss as functions of the plasmonic slot height for different slot widths. The dimension of the dielectric waveguide is still kept at 260 nm×220 nm and the arm separation at 250 nm. It can be seen that strong coupling exists even if the dimensions of the plasmonic waveguide change in a large range. The reason is that the effective refractive index of the plasmonic waveguide is not quite sensitive to the slot dimensions in a large range. Figure 10 shows the effective refractive index and the loss of the decoupled MIM plasmonic waveguide.

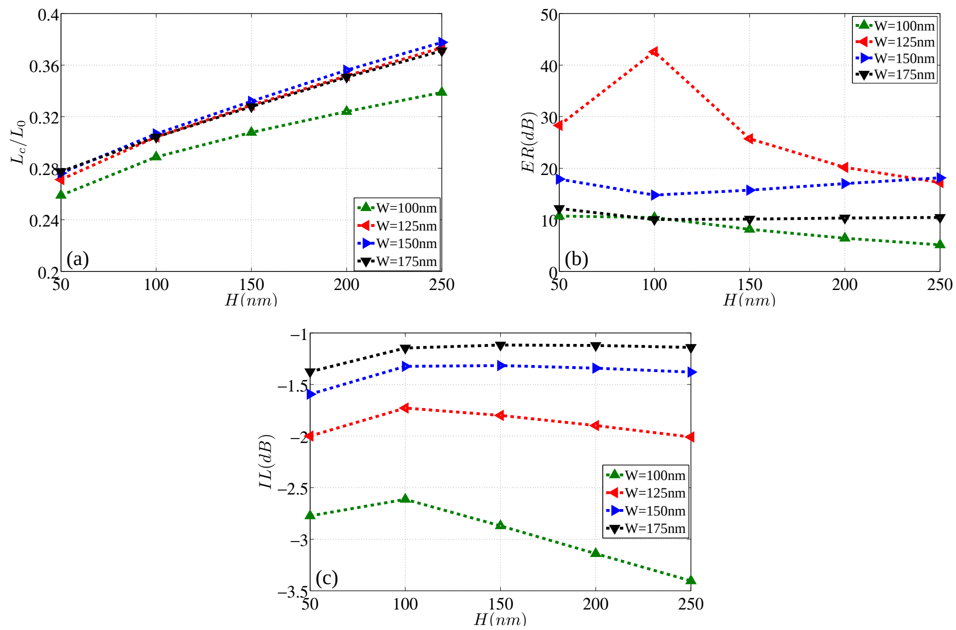

Fig. 9. Tolerance of the hybrid coupler to slot structural parameters. (a)-(c) are the coupling length, extinction ratio (ER) and insertion loss (IL) versus the slot height for different slot widths at *s*=250 nm, respectively.

It can be seen from Fig. 9(a) that the coupling length of the hybrid coupler increases with the slot height. This is because the percentage of the overlapped field between the plasmonic mode and the dielectric mode decreases with the slot height, thereby leading to an increase in the coupling length. In contrast, the coupling lengths are less sensitive to the slot width. The coupling lengths are almost the same for *W*=125 nm, 150 nm and 200 nm because the percentage of the overlapped field doesn't change too much with an increasing slot width. Even at *W*=100 nm, the coupling length decreases by less than 10%.

From Fig. 9(b), the extinction ratios for *W*=100 nm, 125 nm and 150 nm are above 10 dB in the range of interest. Especially, the extinction ratio is above 40 dB at *W*=125 nm and *H*=100 nm where there is almost no residual power in the dielectric arm.

For the insertion loss, it is below 2 dB for *W*=100 nm, 125 nm and 150 nm from Fig. 9(c). From Fig. 10(b), we can see that the propagation loss of the decoupled plasmonic mode increases with a decreasing slot width due to the increase of percentage of field in the metal regions. However, the propagation loss doesn't change too much with the slot height because the percentage of fields inside the slot almost keeps constant. Since the propagation loss dominates the total insertion loss, the insertion loss of the hybrid coupler just follows the trend of the propagation loss for the decoupled plasmonic mode.

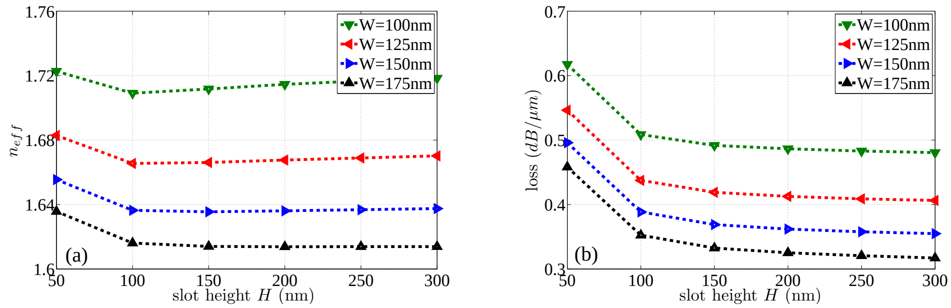

Fig. 10. (a) Effective refractive index and (b) loss of the decoupled MIM plasmonic waveguide versus the slot height for different slot widths.

4.5. Tolerance to the misalignment between the plasmonic waveguide and the dielectric waveguide

For any directional coupler that adopting the vertical coupling configuration, the misalignment between the two waveguides is virtually unavoidable in fabrication. However, the hybrid coupler proposed here is quite tolerant to the misalignment between the plasmonic waveguide and the dielectric waveguide.

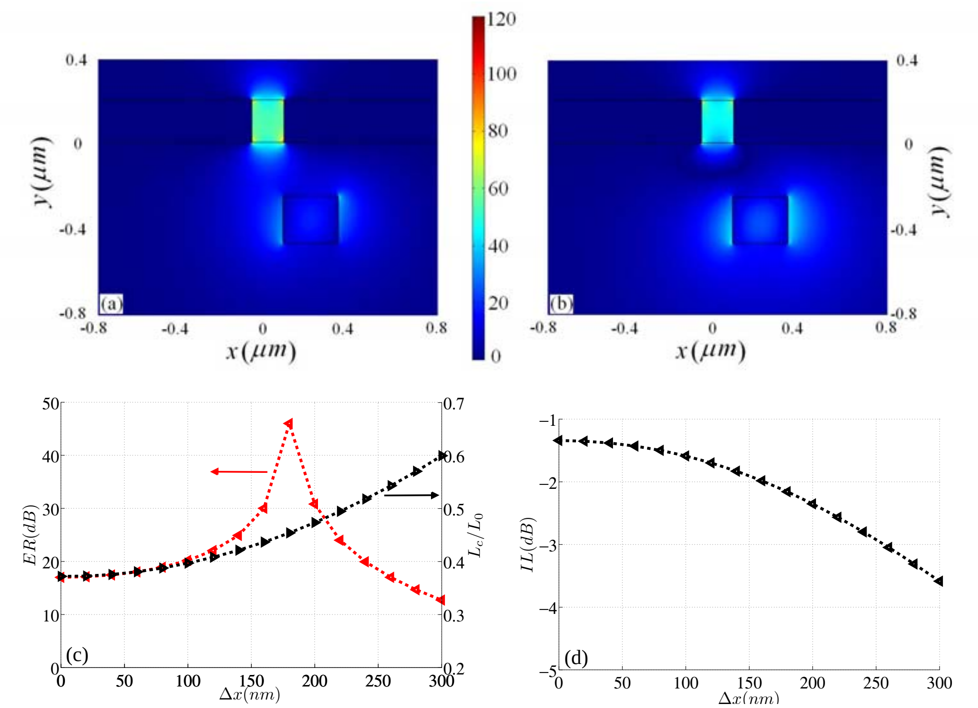

Fig. 11. (a) and (b) are electric field (E_x) amplitudes of the quasi-even mode and quasi-odd mode in the hybrid coupler at Δx=200 nm (s=250 nm), respectively. All the parameters except Δx are the same as those in Fig. 2. (c) Coupling length and extinction ratio (ER) versus the misalignment Δx at s=250 nm. (d) Insertion loss (IL) versus the misalignment Δx at s=250 nm.

Figures 11(a) and (b) provide the electric field (E_x) amplitudes of the quasi-even mode and quasi-odd mode in the hybrid coupler at Δx=200 nm, respectively. Here Δx denotes the misalignment between the two waveguides in the x direction. All the parameters except Δx are the same as those in Fig. 2.

The coupling length and the extinction ratio of the hybrid coupler versus the misalignment Δx are shown in Fig. 11(c). The coupling length increases gradually with an increasing Δx. At Δx=0, the coupling length is $0.4L_0$. For the extinction ratio, it improves with the increasing Δx first and then degrades with the increasing Δx. The change of extinction ratio with respect to the misalignment Δx is quite similar to that with respect to the arm separation s. At small Δx, the unequal excitation of the two eigenmodes degrades the extinction ratio. At large Δx, the degradation of extinction ratio mainly results from the increase in the propagation loss.

The insertion loss of the hybrid coupler versus the misalignment Δx is provided in Fig. 11(d). The insertion loss increases with the increasing Δx, which is mainly caused by the increase in the propagation loss. At Δx=0, the insertion loss is -1.4 dB. At Δx=300 nm, the insertion loss is -3.6 dB.

5. Application of the hybrid coupler as a TM polarizer

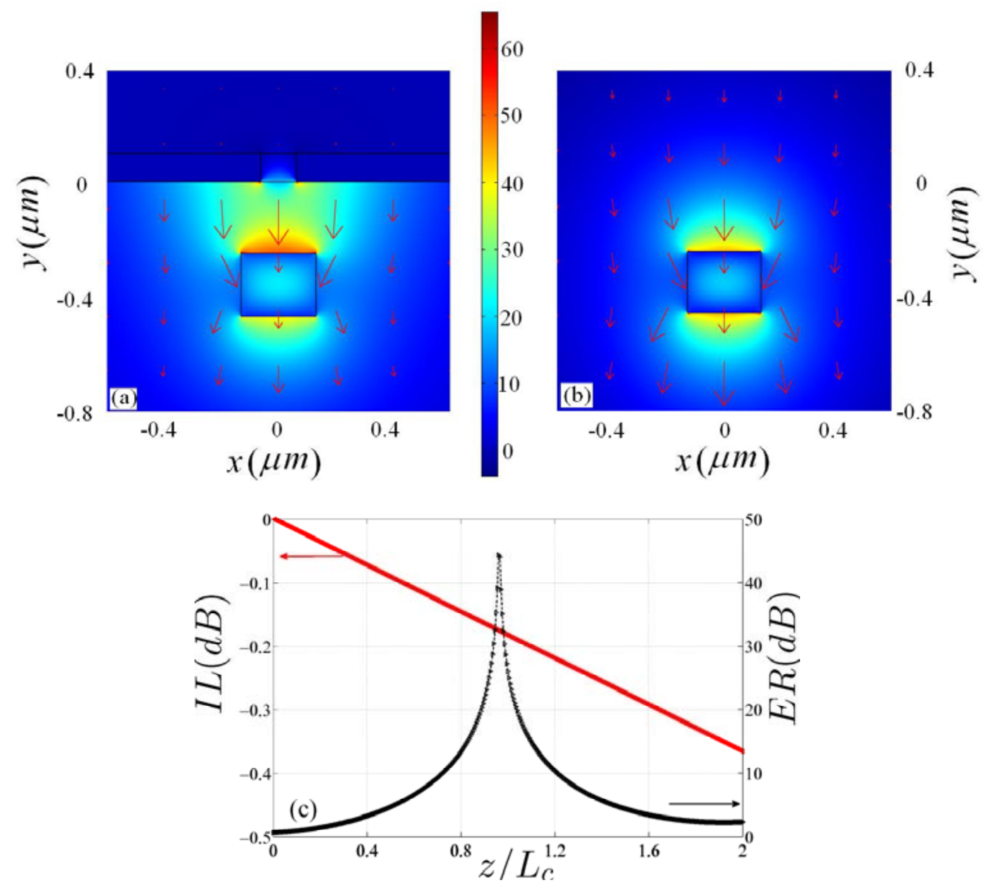

Fig. 12. (a) and (b) are electric field (E_x) amplitudes of TM modes in the hybrid coupler at s=250 nm and the decoupled dielectric waveguide, respectively. (c) Insertion loss (IL) and extinction ratio (ER) of the TM polarizer at s=250 nm.

Since the MIM plasmonic waveguide only support the TE mode, the hybrid coupler can be implemented as a TM polarizer. Figures 12(a) and (b) provide electric field (E_x) amplitudes of the TM modes in the hybrid coupler and the decoupled dielectric waveguide, respectively. To obtain a high extinction ratio, we choose $H2$=100 nm and $W2$=125 nm for the MIM plasmonic arm while the parameters for the dielectric arm keep unchanged. It can be seen that the electric field distributions for the TM mode in the hybrid coupler are quite similar to those in the decoupled dielectric waveguide. A small difference is that the TM fields are truncated by the metal boundaries, which accounts for the loss of the TM mode in the hybrid coupler. The calculated loss of the TM mode in the hybrid coupler is 0.048 dB/μm. When the TE and TM modes are fed into the hybrid coupler from the dielectric arm simultaneously, the TE mode will transfer to the plasmonic arm gradually due to the directional coupling while the TM mode will propagate through the dielectric arm with a low loss. Therefore, by properly choosing the interaction length, the TE and TM modes can be separated at the output end. The loss of TM mode represents the insertion loss here. The extinction ratio of this TM polarizer is defined as the output TM power from the dielectric arm with respect to the residual TE power in the dielectric arm. Figure 12(c) shows the insertion loss and extinction ratio of the coupler versus the interaction length z. When z is close to L_c, the maximum extinction ratio is 44 dB and the insertion loss is -0.18 dB. This hybrid coupler can also be used as a TE/TM polarization splitter or combiner.

6. Conclusion

The characteristics of asymmetrical directional coupling between metal-insulator-metal plasmonic waveguides and dielectric silicon waveguides have been investigated based on the finite element method and the coupled mode theory. The coupling length, extinction ratio and insertion loss of the hybrid coupler have been analyzed. A distinguished feature for this hybrid coupler is that it exhibits high tolerance to the structural parameters of the MIM plasmonic waveguide and the misalignment between the two waveguides, thereby alleviating the stringent requirements in fabrications to some extent. This directional coupler could be potentially exploited for developing photonic-plasmonic hybrid functional components for signal routing, power splitting, wavelength demultiplexing, etc in PICs. In addition, it provides an approach for efficiently exciting MIM plasmonic modes with conventional dielectric modes. Another application of this hybrid coupler is polarization control. TM polarizer, TE/TM polarization combiner, and splitter can be designed based on this hybrid coupler.

7. Acknowledgments

This work is supported by the Swedish Foundation for Strategic Research (SSF) and the Swedish Research Council (VR).